Microearthquake seismicity at the intersection between the Kazerun fault and the Main Recent Fault (Zagros, Iran)

Farzam Yamini-Fard, Denis Hatzfeld, M. Tatar, M. Mokhtari

Geophys. J. Int. (2006) **166,** 186–196 doi: 10.1111/j.1365-246X.2006.02891.x

Microearthquake seismicity at the intersection between the Kazerun fault and the Main Recent Fault (Zagros, Iran)

Farzam Yamini-Fard,[1,2] Denis Hatzfeld,[1] Mohammad Tatar[2] and Mohammad Mokhtari[2]

[1] *Laboratoire de Géophysique Interne et Tectonophysique, CNRS, UJF, BP 53X,* 38041-*Grenoble, France. E-mail: denis.hatzfeld@ujf-grenoble.fr*
[2] *International Institute of Earthquake Engineering and Seismology, PO Box* 19395/3913*, Tehran, Iran*

Accepted 2005 December 18. Received 2005 October 26; in original form 2005 April 4

SUMMARY

Seismicity and fault plane solutions of earthquakes at the intersection between the Main Recent Fault (a right-lateral strike-slip fault that bounds the Zagros to the NE) and the Kazerun Fault system (another right-lateral zone that crosses the Zagros) show slip to be partitioned into nearly pure strike-slip at shallow depths and nearly pure thrust slip below 12 km. Such slip partitioning is commonly observed where oblique convergence occurs, but in general faults of different styles lie adjacent to one another, not at different depths with one below the other. We provide evidence for this partitioning in a microearthquake study in which we deployed a temporary network of 29 seismographs for 7 weeks. We located no activity north of the Main Zagros Reverse Fault (MZRF), which separates the Zagros fold belt from Central Iran. Most earthquakes occurred between the northern termination of the Kazerun Fault and the MZRF, but not near to known major faults. Activity is limited to the upper crust, between 2 and 16 km. Most of the focal mechanisms show strike-slip faulting, dextral if the NS striking plane is the active plane, but a few for the deepest events show reverse faulting, distributed between the Kazerun Fault and the MZRF, with *P*-axis trending consistently ∼NS. This partitioning of the deformation with depth suggests that the brittle upper crust deforms by slip on pre-existing faults that strike obliquely but that the lower crust accommodates the shortening by reverse faulting. We infer that the deformation in the upper part of the crust reflects a stiffer medium in which pre-existing faults localize the deformation. The largest event recorded during this experiment, located at the same place as the destructive 1977 Naghan earthquake (Mw ∼5.9, 348 victims), shows reverse faulting, likely related to the Dopolan High Zagros Fault. The crustal thickness deduced from receiver function analysis does not show a marked difference across the Kazerun fault, which suggests a pure strike-slip motion on the fault.

Key words: focal mechanisms, partitioning, Iran, Kazerun, microseismicity, Zagros.

INTRODUCTION

In regions of oblique convergence, slip between converging blocks commonly is partitioned into nearly pure thrust faulting on some faults and nearly pure strike-slip faulting on nearly parallel faults (e.g. Fitch 1972; McCaffrey 1992). Perhaps the simplest explanation for this pattern is that near the Earth's surface principal stresses must be horizontal or vertical, and oblique slip is not favoured (Richard & Cobbold 1989). To the best of our knowledge, such partitioning on faults at different depths is not commonly observed, but we report such a result here for a section of the Zagros where oblique convergence occurs and strike-slip faults are clear at the surface.

The NW–SE trending Zagros mountains form a linear belt more than 1200 km in length, from Eastern Turkey in the NW to the Strait of Hormuz in the SE (Fig. 1). They result from the continental collision between the Arabian plate and Central Iran that started during the Miocene (e.g. Stöcklin 1968), or perhaps earlier in Cenozoic time. At the present time, shortening across the Zagros accommodates about 30–50 per cent of the ∼25 mm y^{-1} convergence between Arabia and Eurasia (Tatar *et al.* 2002; Vernant *et al.* 2004). The Zagros is bounded to the north by the Main Zagros Reverse Fault (MZRF), which is considered to have been the active thrust fault between Arabia and Iran during subduction and before suturing occurred (i.e. Falcon 1974). Both the absence of seismicity (Tatar *et al.* 2004) and the lack of deformation revealed by repeated GPS measurements (Tatar *et al.* 2002) show that this is not currently active.

The Kazerun–Borazjan Fault system belongs to a wide zone of NS striking right-lateral discontinuities of pre-collisional origin (i.e. Falcon 1969) and includes the Karebas, Sabz Pushan, and Sarvestan transfer zones (Ricou *et al.* 1977; Berberian 1995; Talebian & Jackson 2004; Authemayou *et al.* 2005). This fault system obliquely crosscuts the entire width of the Zagros.

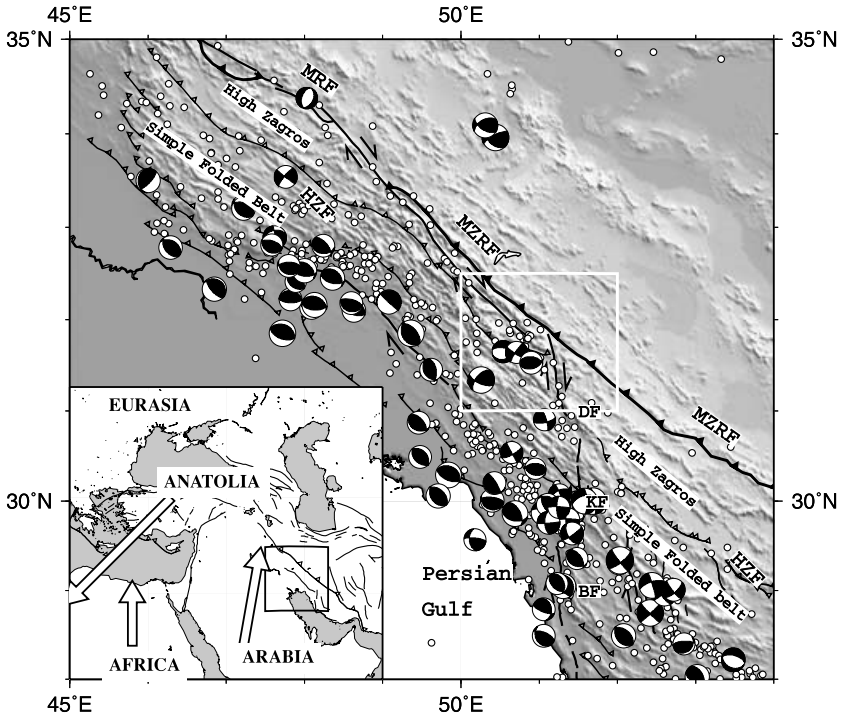

Figure 1. Map of the Zagros mountain belt with instrumental seismicity re-located by Engdahl *et al.* (1998) and CMT focal mechanisms (http://www.seismology.harvard.edu/CMTsearch.html). The main faults are those given by Talebian & Jackson (2004). The area of study is the white square located at the intersection between the Kazerun fault system and the Main Recent Fault. The inset shows the geodynamic frame of the Arabian-Eurasian collision.

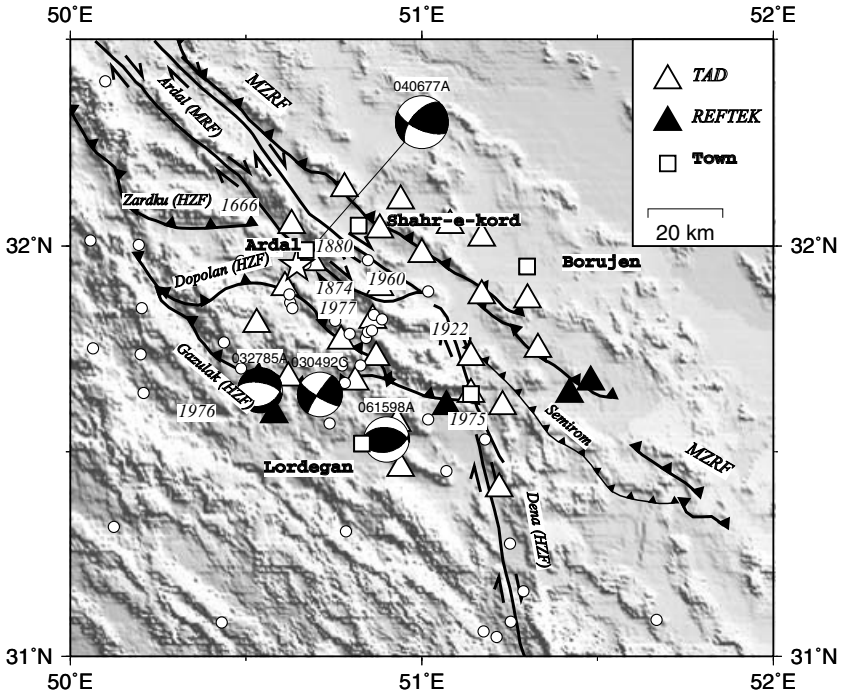

Figure 2. Map of the temporary local network deployed in the region of Borujen from 17 April, 2002 to 11 June, 2002. The main faults and the main cities (squares) are from Berberian (1995) and Authemayou *et al.* (2005). We show the historical seismicity with their year in a box (Ambraseys & Melville 1982; Berberian 1995) and the CMT solutions. We show the instrumental seismicity (Engdahl *et al.* 1998) as white circles. The star is the location of the 1977 Naghan destructive earthquake. The single-component seismological stations are depicted by empty triangles and the three-component seismological stations by black triangles.

Table 1. Velocity structure.

Top layer km	Velocity km s^{-1}
00.0	5.30
08.0	5.90
14.0	6.20

East of the Kazerun–Borazjan Fault system, the Zagros Fold Belt is relatively wide, strikes perpendicular to the orientation of the convergent motion, and is affected by numerous salt extrusions. Shortening there occurs by distributed reverse faulting within the belt (e.g. Berberian 1995). The eastern Zagros accommodates shortening of only about 1 cm yr^{-1}, perpendicular to the folded structures (Berberian 1995; Talebian & Jackson 2004; Tatar *et al.* 2004). West of the Kazerun–Borazjan Fault system, the Zagros mountains form a narrower belt that strikes obliquely to the orientation of convergence. The convergence is accommodated by partitioning between (a) shortening (thrust-and-fold belt) that seems to be distributed across the belt and perpendicular to it and (b) strike-slip motion located on the Main Recent Fault, a NW–SE striking right-lateral strike-slip fault parallel to the belt and to the MZRF (Tchalenko & Braud 1974; Koop & Stoneley 1982; Berberian 1995; Talebian & Jackson 2002; Authemayou *et al.* 2006).

Estimates of the right-lateral total offset along to the Kazerun–Borazjan Fault system Fault range from as much as 140 km (Berberian 1995) to less than 30 km (Authemayou *et al.* 2006). It consists of three distinct strike-slip fault zones striking NS: the Dena, Kazerun, and Borazjan Faults. The southern termination of each fault curves towards the east to become a reverse fault (Authemayou *et al.* 2005). The Kazerun–Borazjan Fault system accommodates the differential shortening between northwestern and southeastern Zagros. It transfers and distributes the strike slip along the Main Recent Fault, which occurs parallel to the orogen, to the southeastern Zagros where it manifests itself as a fold-and-thrust belt perpendicular to the orientation of shortening (Authemayou *et al.* 2006). The Kazerun Fault system is clearly associated with right-lateral strike-slip earthquake focal mechanisms (Baker *et al.* 1993).

The connection between the Kazerun Fault system (locally the Dena fault) and the Main Recent Fault (locally the Ardal Fault) lies near the city of Borujen (Berberian & Navai 1977; Ricou *et al.* 1977; Authemayou *et al.* 2005).

Destructive historical or instrumental earthquakes occurred in 1666, 1874 and 1880 near the Ardal Fault and in 1934, 1975 and 1989 near the Dena Fault (Fig. 2), but the associated focal mechanisms are not clear (Berberian, 1995). Seismic activity is low in the High Zagros, and it is bounded to the east by the Dena Fault and to the north by the MZRF (Figs 1 and 2). The Naghan earthquake of 1977 April 6 ($Mw \sim 5.9$, 348 victims), the largest earthquake recorded teleseismically from this area, occurred beneath the Ardal strike-slip fault, but no surface rupture was observed (Berberian & Navai 1977). The epicentre is located in the area of maximum intensity (which might be biased by a non-uniform distribution of the villages) and the depth is less than 10 km (Engdahl *et al.* 1998). Body-wave modelling of this earthquake (Baker 1993; Talebian & Jackson 2004) shows a well-constrained reverse mechanism with a large component of strike-slip (right lateral on a WNW–ESE striking plane) at a depth of 6 ± 4 km.

Several other strong events have occurred in the area of Borujen. The earthquake of 1975 September 21 ($mb = 5.2$) that destroyed the village of Sarpir was located near the intersection of the High Zagros Fault and the Dena Fault (Berberian & Navai 1977). The earthquake of 1985 March 27 ($mb = 5.1$) is located by NEIC near the High Zagros Fault with a depth of 84 km and a normal faulting mechanism, but Engdahl *et al.* (1998) relocated the same event near the Main Front Fault within the crust. Moreover, Maggi *et al.* (2000) modelled the body-waves and favour a thrust faulting mechanism at shallow depth (10–15 km). The Dashte-Armand earthquake of

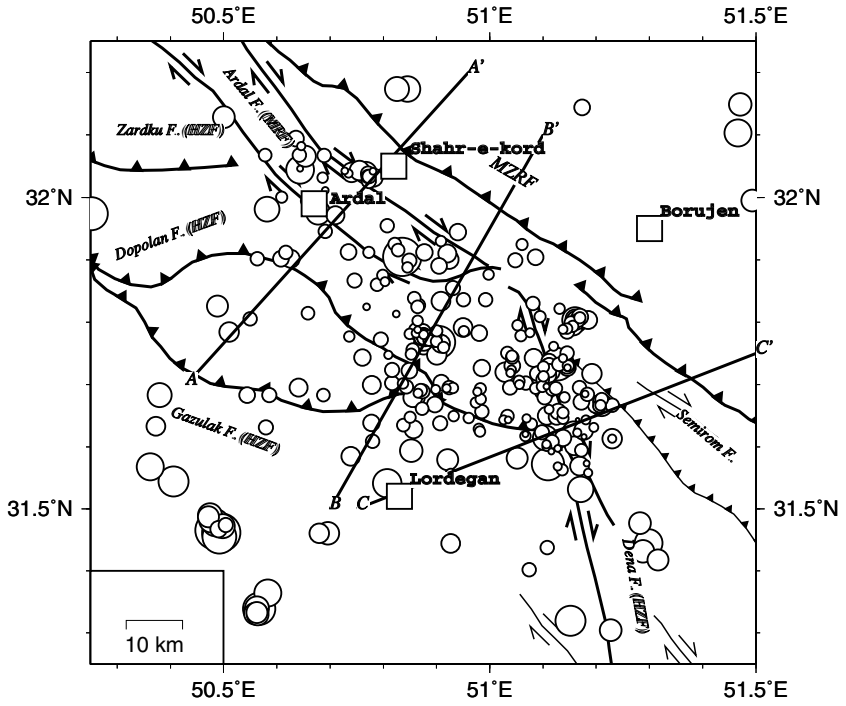

Figure 3. Map of all the 325 events (minimum 3 *P* and 2 *S*) located in the region of Borujen from 2002 April 17 to June 11. We show the locations of the three cross-sections of Figs 6–8.

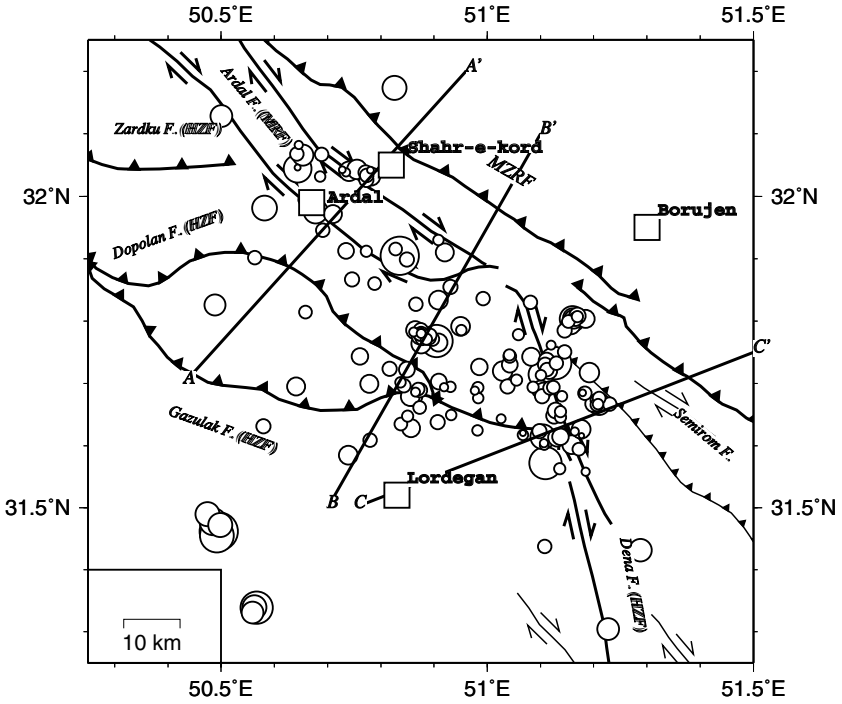

Figure 4. Map of the 144 selected events (RMS ≤ 0.2 s, ERH and ERZ ≤ 2 km, $N > 6$). The majority of events are located around the Ardal and Dena Faults.

1992 March 4 ($mb = 4.9$) near the High Zagros Fault is associated with a strike-slip fault. The 1998 June 15 ($mb = 4.9$) earthquake located near this fault occurred by reverse slip on an EW striking fault. The earthquake of 1998 September 21 ($mb = 5.2$), near the Dena Fault shows a strike-slip mechanism. Thus, the mixture of strike-slip and reverse mechanisms in this area with consistent N–S trending *P* axes concur with the orientation of shortening deduced from both tectonics and GPS measurements.

We installed a temporary network of seismographs surrounding the intersection between the Kazerun Fault and the Main Recent Fault to study the internal deformation in that place.

DATA AND RESULTS

From 2002 April 17 to June 11, we operated 29 seismological stations in the area of Borujen (Fig. 2). The network covered the MZRF, the Ardal fault (eastern termination of the Main Recent Fault), and the Dena fault (northern termination of the Kazerun fault). The instruments were 25 1 Hz vertical Mark-Product seismometers connected to TAD digital recorders working in a trigger mode and four three-component CMG40 broad-band seismometers connected to Reftek data loggers recording continuously. The sampling rate was 100 samples per second, and time was monitored by a GPS receiver in each station.

Velocity structure

Among the total number of 325 earthquakes that we could locate, we select 88 events with a minimum of 6 *P* or *S* phases ($N \geq 6$), a root-mean-square (RMS) residual ≤0.1 s, calculated horizontal (ERH) and depth (ERZ) uncertainties ≤1 km, and a GAP in azimuthal coverage ≤180°, which we use to search for the appropriate velocity structure. First, averaging Tsj-Tsi versus Tpj-Tpi for all events and all stations, we compute a *Vp*/*Vs* ratio of 1.85 ± 0.02 with a total number of 423 arrival times. This relatively high value may be due to a *Sp* conversion at a shallow depth read on the vertical component seismometers. Second, we determine the velocity structure by applying two different methods: (a) we explore three-layer models (varying the thickness and the velocity of all layers) by minimizing the residuals, and (b) we perform a 1-D inversion of the arrival times using the VELEST program (Kissling 1988) in to steps. In order to check for the convergence of the inversion to a unique velocity structure we generate a set of 50 initial models by introducing random changes (up to 0.5 km s^{-1}) for each layer of the model that minimizes the residuals. First, we start with an initial model composed of a stack of layers 2 km thick of uniform velocity 6.0 km s^{-1}. This close spacing of layers allows us to determine the approximate depths and magnitudes of the main velocity contrasts but does not allow convergence to a simple, sensible structure because of the large number of unknown quantities. It does, however, suggest that a three-layer model is appropriate with two velocity contrasts located at 8 and 15 km depth. We then use a three-layer model, with such contrasts, as the second initial model and randomly perturb it to get the final model given in Table 1, which, we think looking at the scatter, is uncertain by 0.1 km s^{-1} for the top layer and 0.3 km s^{-1} for the bottom layer. Because we invert separately for *S* and *P* arrival times, we were able to confirm a high *Vp*/*Vs* ratio (greater than 1.80) in all the three layers.

Distribution of epicentres

We locate (Fig. 3) a total number of 325 events (with a minimum of 3 *P* and 2 *S*), of magnitude *Ml* ranging from 0.5 to 4.0, using the Hypo71 software (Lee & Lahr 1975). For most RMS residuals are less than 0.2 s, and calculated uncertainties in both epicentre and depth are less than 2 km (Yamini-Fard 2003). Most of the seismic activity is located between the region surrounded by the MZRF to the north, Dena Fault to the east, and Zardku Fault to the south. However, it is clear that no earthquake occurred on the MZRF. We do observe

Table 2. Parameters of the focal mechanisms.

num	date	heure	lat	lon	prof	mag	Az1	pl1	de1	Az2	pl2	de2	Azp	dep	Azt	det	Im	Q
25	020423	21:40	31.667	51.210	13.90	2.1	65.0	85.0	90.0	245.0	5.0	90.0	155.0	40.0	335.0	50.0	1	B
26	020423	21:46	31.667	51.200	13.98	1.6	90.0	85.0	90.0	270.0	5.0	90.0	180.0	40.0	360.0	50.0	1	B
59	020501	10:22	31.834	50.908	6.04	1.8	75.0	83.0	35.7	340.0	54.6	171.4	202.4	18.9	303.6	29.7	1	B
69	020503	08:54	31.976	50.678	12.84	2.3	45.0	75.0	18.7	310.0	72.0	164.2	177.1	2.0	268.0	23.7	1	C
81	020505	23:26	31.733	51.128	8.91	3.1	70.0	75.0	7.7	338.0	82.6	164.9	24.7	5.3	293.2	15.9	1	B
95	020507	05:53	31.714	51.101	10.15	2.4	80.0	65.0	22.6	340.0	69.6	153.2	30.8	3.0	298.9	33.1	1	B
122	020510	21:35	31.623	51.098	10.41	1.4	95.0	45.0	90.0	275.0	45.0	90.0	185.0	.0	90.0	90.0	1	C
126	020511	16:52	31.791	50.950	11.98	1.8	60.0	75.0	34.3	320.0	57.1	162.0	186.6	11.6	284.8	34.6	1	C
164	020517	04:29	31.900	50.924	11.57	1.8	30.0	65.0	−168.3	295.0	79.4	−25.5	250.0	25.4	344.6	9.7	−1	C
193	020522	03:29	32.044	50.644	7.13	2.7	30.0	75.0	−18.7	125.0	72.0	−164.2	347.0	23.7	77.9	2.0	−1	C
226	020526	23:24	31.688	51.105	11.58	1.6	35.0	65.0	11.7	300.0	79.4	154.5	349.6	9.7	255.0	25.4	1	A
227	020526	23:35	31.764	50.876	5.50	1.9	210.0	80.0	−153.3	115.0	63.7	−11.2	75.4	25.9	340.0	11.0	−1	A
228	020527	00:35	31.690	51.101	6.01	1.7	140.0	75.0	145.7	240.0	57.1	18.0	193.4	11.6	95.2	34.6	1	A
232	020527	15:36	32.173	50.826	6.63	2.3	100.0	75.0	90.0	280.0	15.0	90.0	190.0	30.0	10.0	60.0	1	C
237	020527	23:51	31.803	51.160	10.55	2.5	80.0	65.0	22.6	340.0	69.6	153.2	30.8	3.0	298.9	33.1	1	A
262	020530	14:21	31.747	50.901	13.17	1.9	70.0	75.0	18.7	335.0	72.0	164.2	202.1	2.0	293.0	23.7	1	C
275	020601	03:05	31.743	51.042	10.86	1.2	45.0	65.0	11.7	310.0	79.4	154.5	359.6	9.7	265.0	25.4	1	C
298	020604	06:02	31.904	50.835	13.56	3.7	90.0	65.0	90.0	270.0	25.0	90.0	180.0	20.0	.0	70.0	1	A
317	020609	14:17	31.981	50.582	20.19	2.4	55.0	80.0	26.7	320.0	63.7	168.8	185.0	11.0	280.4	25.9	1	B

a significant seismic activity around the northern termination of the Dena Fault and the eastern termination of the Ardal Fault (part of the Main Recent Fault), but the relationship of this seismicity to these faults is unclear. We cannot map precisely the locations of active faults or infer the sense of motion of possibly active faults.

To refine the tectonic interpretation, we select the 144 events with a RMS residuals $\leq$0.2 s, both ERH and ERZ $\leq$2 km, and an azimuthal gap $\leq$270° and recorded with a minimum of 6 phases (Fig. 4). The limitation on the azimuthal gap eliminates events located outside the network, and the picture that we now obtain is valid only within, or close to, the seismological network. Only one event is located north of the MZRF and, as noted above, no earthquake is located on the fault itself. The seismicity is concentrated near the Dena Fault and on the Ardal Fault, but again it is not possible to map linear patterns possibly related to single active faults. The depths of these 144 events range between 2 and 16 km, within the upper crust and, therefore, shallower than in the Central Zagros (Tatar *et al.* 2003).

In order to precisely locate the active fault planes, we relocate the earthquakes with the Double Difference algorithm HypoDD (Waldhauser and Ellsworth 2000), which allows better relative location within clusters of earthquakes when the velocity structure is not accurately known (Fig. 5). We use parameters (minimum arrival times for one event, distance between events within a cluster) that

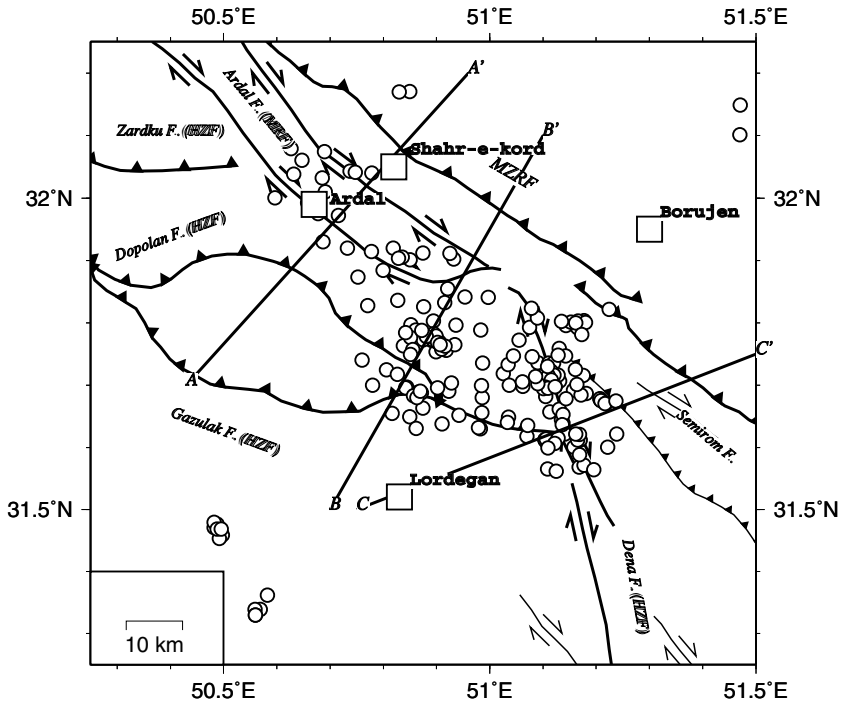

Figure 5. Map of the 140 events located using the double-difference technique (Waldhauser and Ellsworth 2000) in order to overcome any bias due to unknown velocity heterogeneities.

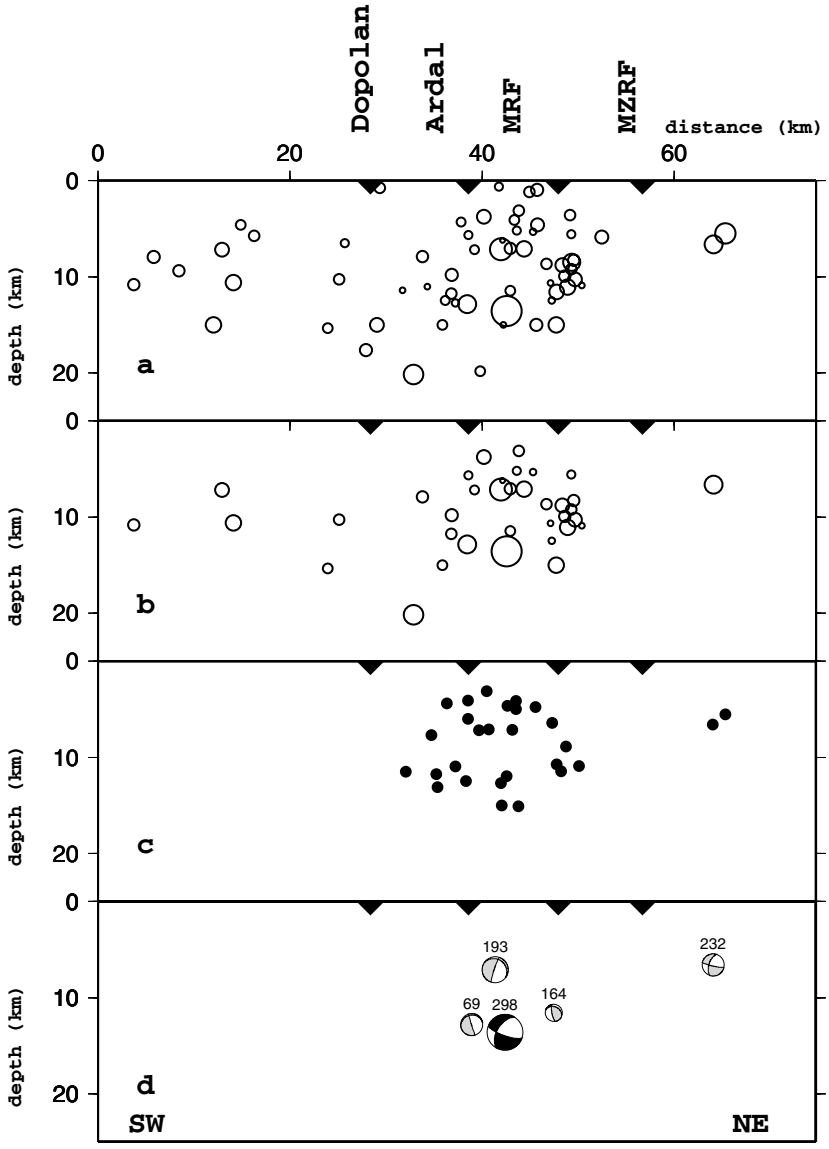

Figure 6. Cross-section across the Ardal Fault (A–A′ in Fig. 3). (a) from the total set of 325 events, (b) from the 144 selected events, (c) from the 140 double-difference re-located events and (d) back-hemisphere projections of focal mechanisms projected onto the section. Black mechanisms are of quality A, dark grey of quality B, light grey of quality C (see text.). The width of the section is 40 km. The different faults are reported on the top.

do not separate the seismicity into many narrow clusters, but allow us to relocate most events relative to each other. Among the total number of 325 events, 202 events were considered to be clustered and 179 occurred within a single cluster (Fig. 5). The relocation slightly reduces the scatter in seismicity, mostly around the northern termination of the Dena Fault. However, HypoDD is efficient for clusters, which is not really the case in our data and, therefore, we do not expect a significant improvement.

To constrain the geometry of possible active faults, we plot 3 different cross-sections perpendicular to the major tectonic structures in this area. A NE–SW striking cross-section in the western part of the Ardal Fault (Fig. 6) does not provide any evidence for a pattern with depth. A NNE–SSW striking cross-section of the easternmost part of the Ardal Fault (Fig. 7) suggests a vertical cluster of earthquakes located slightly south of the Ardal Fault. This cluster dips almost vertically, but its extension along strike lies at depths less than 10 km (Fig. 5), which limits the interpretation in terms of a vertical strike-slip fault. The third cross-section trends NE–SW across the northern termination of the NS striking right-lateral Dena strike-slip fault (Fig. 8). Seismicity (especially the HypoDD relocated earthquakes) dips vertically beneath the Dena Fault, but the horizontal dimension of the cluster is only ∼10 km, considerably less than the length of the fault. Therefore, the association with a vertical strike-slip fault is uncertain.

Focal mechanisms

We calculate 19 focal mechanisms with a minimum of six first motion polarities and an azimuthal gap of less than 45° (Fig. 9 and Table 2). We separate the solutions within 3 different categories depending on their reliability. Category A (5 mechanisms: (#226, 227, 228, 237, 298) includes solutions with three quadrants sampled by first motion polarities. In category B are solutions with two quadrants well sampled and uncertainties in the orientations of the planes

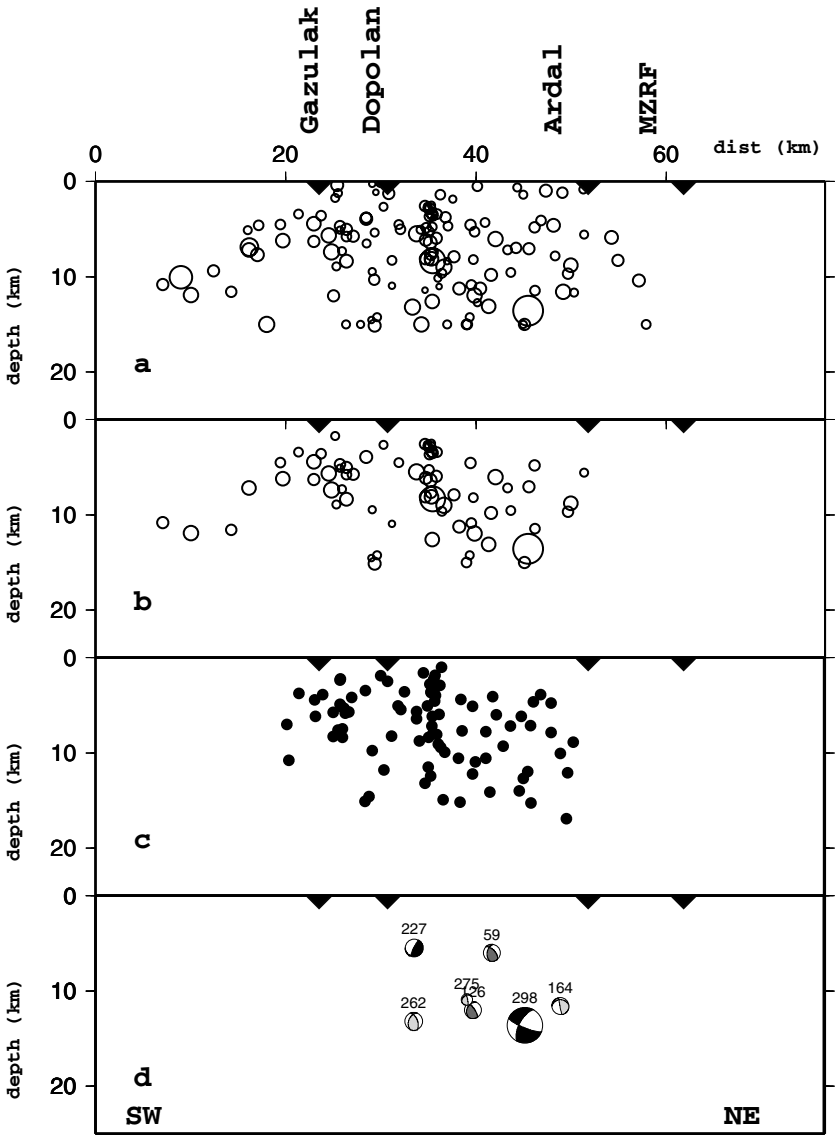

Figure 7. Cross-section across the southern Ardal Fault (B–B′ in Fig. 3). Same symbols as in Fig. 6.

less than 20°. Category C contains mechanisms with quadrants well sampled but without redundant polarities and, therefore, are least reliable.

Three mechanisms in category A (#226, 228, and 237) show right-lateral strike slip (assuming the NNW–SSE trending fault plane) probably related to the Dena Fault. For #227, located close to the Ardal Fault, slip is left-lateral, if we choose the NW–SE plane to be fault plane, which is inconsistent with the tectonics in this area. The solution is consistent with a NNE-SSE striking right-lateral faulting between the HZF and the Ardal Fault.

The largest event recorded during this experiment, #298, of magnitude 3.7 and located north of the Ardal Fault at a depth of 14 km, shows reverse faulting. It was felt by the majority of the population living in this region. Moreover, this event occurred within the region of maximum intensity of the 1977 April 6 Naghan earthquake (Ms, 6.0) that was not followed by aftershocks (Berberian & Navai 1977). This reverse mechanism is not consistent with the strike-slip motion of the Ardal fault. Located at a depth of 14 km, however, it could reflect slip on either the Gazulak or the Dopolan reverse faults that crop out at the surface farther south. Using a synthesis of body waves Baker *et al.* (1993) shows that the 1977 earthquake occurred by reverse faulting with a right-lateral strike-slip component and a hypocentre at a depth of 6 km, inconsistent with the less reliable depth of 11 km determined by Engdahl *et al.* (1998). The similarities between the 1977 earthquake and the earthquake #298 suggest that the Nagan earthquake was located not on the Ardal fault, but more likely on the Dopolan or the Gazulak reverse faults.

For mechanisms of category B and C, we again observe both strike-slip and reverse mechanisms. Strike-slip mechanisms for earthquakes located near the Ardal Fault (#59, 69, 126 and 193) are right-lateral assuming the NW–SE trending fault plane. One noticeable exception is #164 whose mechanism is similar to that of #227 and suggests slip on the conjugate strike-slip fault striking NE–SW. Strike-slip mechanisms of earthquakes near the Dena Fault (#81 and 95) are also right lateral, if rupture occurred on the plane parallel to the fault. East of the Dena Fault, we observe three reverse-slip mechanisms (#25, 26 and 122) with nodal planes striking obliquely to the Dena fault. All earthquakes showing reverse mechanisms occurred deeper (up to 14 km) than those with strike-slip mechanisms.

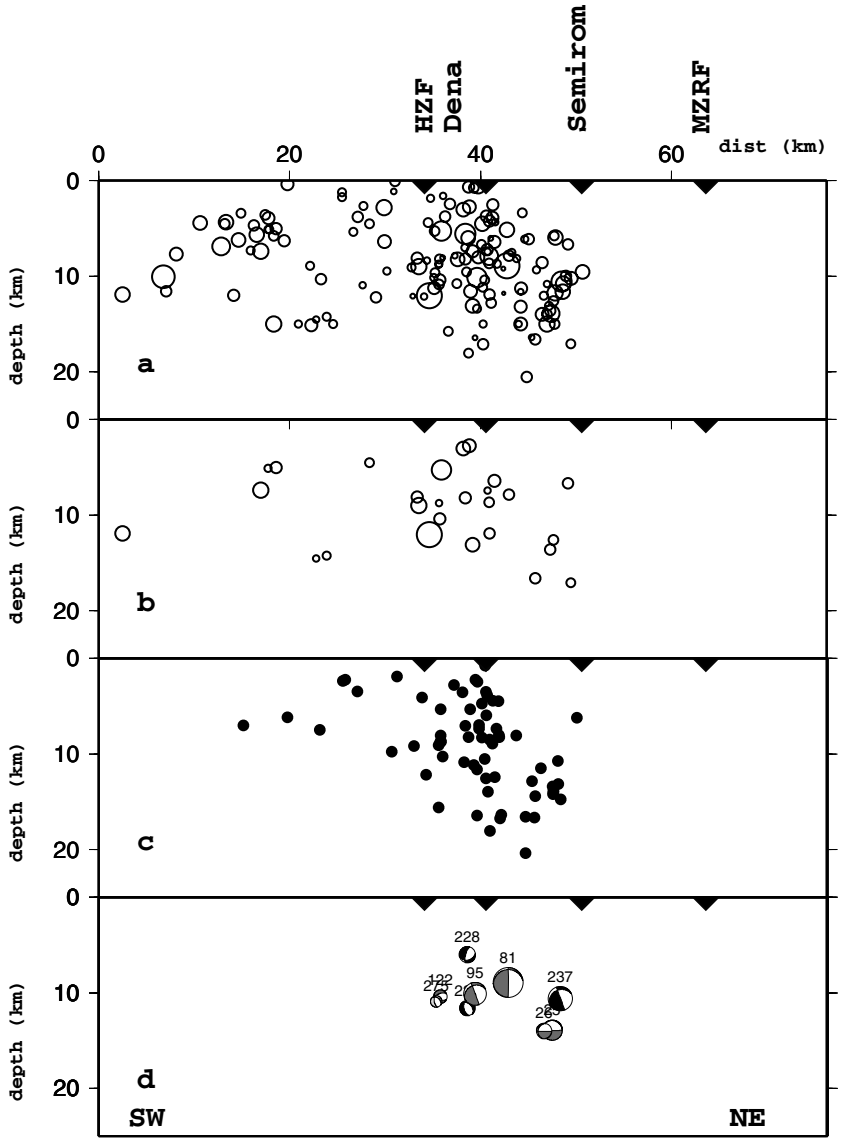

Figure 8. Cross-section across the Dena Fault (C–C′ in Fig. 3). Same symbols as in Fig. 6.

Crustal thickness

During our experiment, we installed four broad-band seismological stations across the Dena fault (Fig. 2) in order to study the crustal thickness on both sides of the Dena fault computing the receiver function of teleseismic earthquakes. We recorded a total number of 29 events of magnitude greater than 5.4 at epicentral distances between 25° and 95°. Only some of these events (between 1 and 13 at each station) were suitable for computing a receiver function, which does not allow us to conduct a extensive study of crustal thickness but can give some indication of it. We used iterative deconvolution in the time domain (Ligorria & Ammon 1999), after rotating the horizontal components into a Radial-Transverse reference frame and applying a Butterworth bandpass filter between 0.05 and 0.8 Hz. Stacking the available receiver-functions for each station, we obtain a strong pulse on the radial component at ∼7 s (Fig. 10). At most stations, the corresponding transverse component is free of a signal, which suggests that we can rely on the quality of the radial receiver function. Indeed we have not many data for the stations KALA and KOLV located west of the Dena fault, but the receiver functions are reasonably clear. Using a mean velocity of 6.0 km s^{-1} and a *Vp*/*Vs* ratio of 1.73, we estimate the crustal thickness to be approximately 55–60 km with no large differences among the four broad-band stations.

DISCUSSION

The purpose of this study was to constrain the mechanism that accommodates motion between the northern part of the NS striking right-lateral strike-slip Kazerun fault system (locally called the Dena Fault) and the eastern part of the NW–SE striking right-lateral strike-slip Main Recent Fault (locally called the Ardal Fault). We also sought to relate the destructive 1977 Naghan earthquake to the active deformation of this region.

Velocity structure across the Kazerun fault

The velocity structure of the upper crust in this region includes a 6–8 km thick sedimentary layer ($Vp \sim 5.3$ km s^{-1}) over a 6 km thick

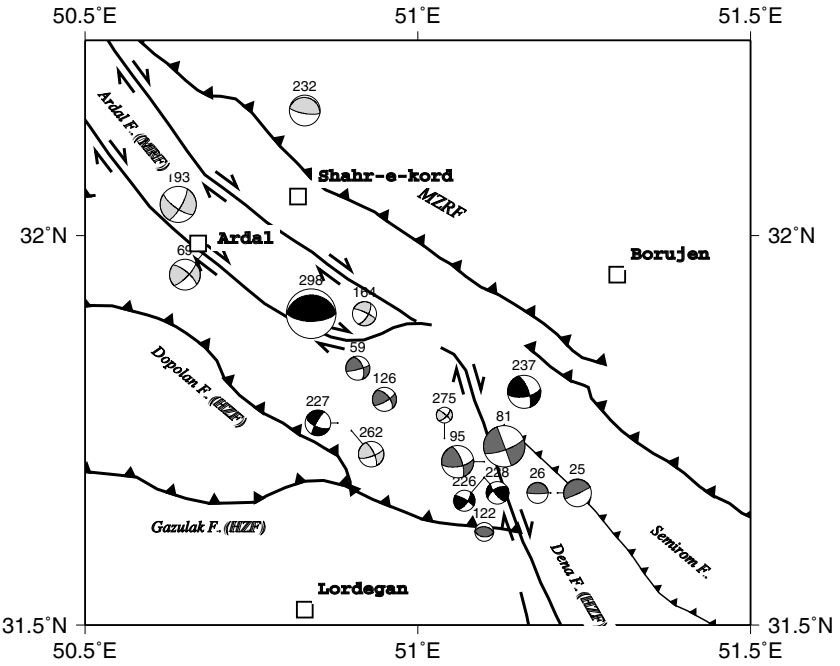

Figure 9. Map of the focal mechanisms. Black mechanisms are of quality A, dark grey of quality B, light grey of quality C (see text.).

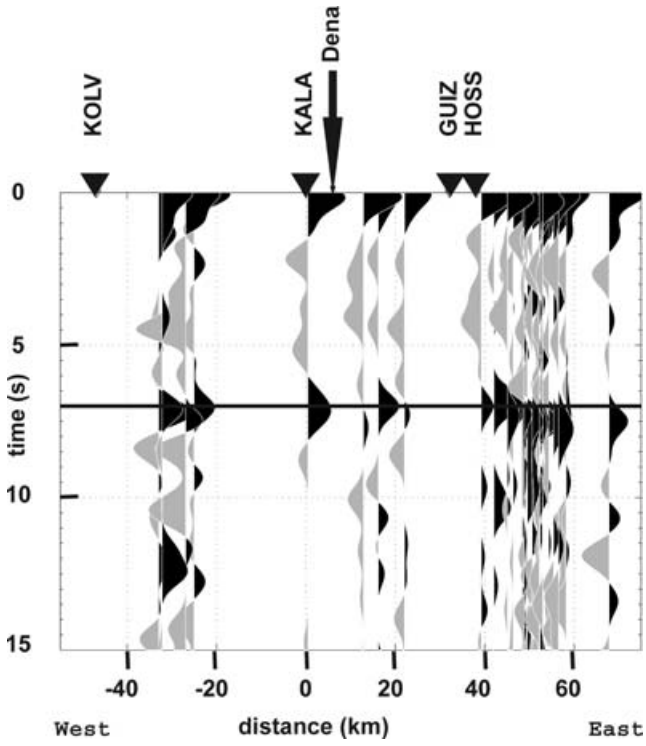

Figure 10. Stack of the teleseismic receiver functions recorded in all four stations equipped with CMG40 broad-band seismometers. The receiver function is computed using the iterative deconvolution of Ligorria & Ammon (1999) after rotating the horizontal components into a Radial-Tranverse reference frame. At all stations we observe a strong pulse at ∼7 s that can be associated with a *Ps* conversion at the Moho. Assuming a *Vp*/*Vs* ratio of 1.73, we can infer a crustal thickness of ∼55–60 km on both sides of the Dena fault.

crystalline layer ($Vp \sim 5.9$ km s^{-1}). This differs from the 11 km-thick layer of 5.0 km s^{-1} obtained by Hatzfeld *et al.* (2003) for the Central Zagros and suggests a more rigid and a thinner sedimentary cover in the High Zagros region. The 60-km-deep Moho inferred from receiver functions is greater than the 48 km obtained for the Central Zagros (Hatzfeld *et al.* 2003) but is close to the value obtained by Kaviani (2004) north of Main Zagros Thrust. We find no marked difference, larger than several km, of the crustal thickness across the Kazerun Fault, which suggests that the blocks east and west of the fault have the same origin. Thus the Kazerun fault system acts as a nearly pure strike-slip fault offsetting two crustal blocks of similar thickness, in contrast with the MZRF, which marks the location of the former subduction and subsequent crustal thickening.

Activity of the MZRF

We observed no seismicity related to the MZRF and, thus, this feature does not seem to behave as an important kinematic discontinuity at present, as confirmed by GPS observations (Walpersdorf *et al.* 2006). Seismicity is diffuse, confined to the south of this reverse fault, and is mostly concentrated along and between the Ardal, Dena, and High Zagros faults. The microearthquake seismicity does not define a clear trend, nor does it show a clear relationship with known active faults, but there is certainly a concentration of the seismicity near the intersection of the Dena Fault and the Ardal Fault. This complex pattern of seismicity is not surprising because our study was located at the intersection of several faults, both strike-slip and reverse, that have been inherited from previous tectonic episodes. From the cross-section located at the east of the Ardal fault, we infer that seismicity is associated with either the Dopolan or the Gazulak NNE dipping faults (Fig. 7). We also suggest that the reverse mechanism #298, which is located at 14 km depth, is associated to one of these faults. Moreover, from the cross-section located across the Dena fault (Fig. 8), we confirm that seismicity is likely to be associated with the Dopolan of the Gazulak reverse faults dipping

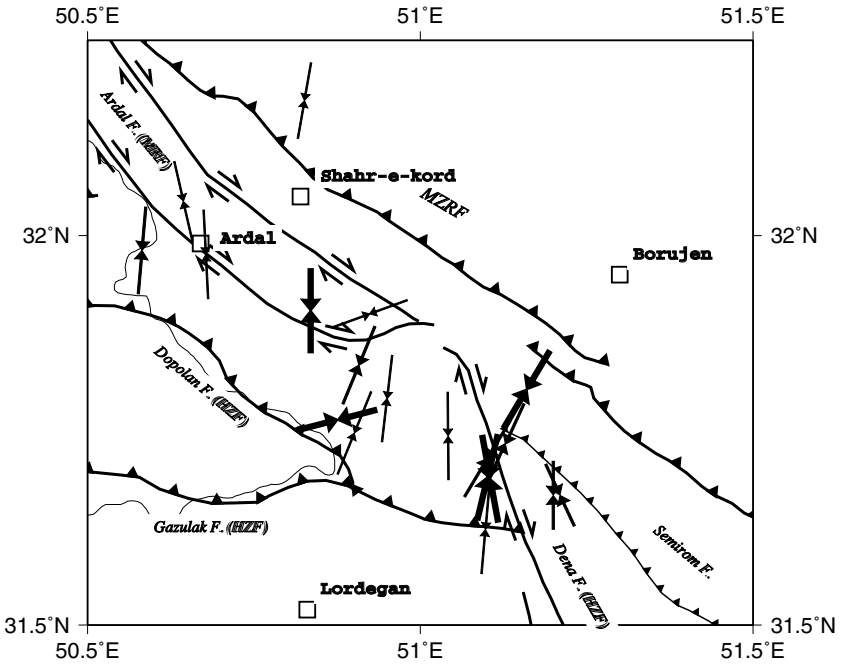

Figure 11. Map of the *P* axes deduced from the focal mechanisms. Heavy arrows are for quality A, middle for quality B, thin for quality C (see text).

northeastwards. Only rare seismicity is associated with, or located northeast of, the Semirom fault (Figs 3–5), located east of Borujen, and which is proposed to partially share the transfer of motion with the Kazerun fault (Authemayou *et al.* 2005).

Partitioning of deformation

Focal mechanisms include both reverse faulting (on faults striking ∼EW) and strike-slip faulting, but the *P*-axes trend consistently ∼NS, independently of the type of faulting (Fig. 11). For the more tightly constrained mechanisms of category A and B, the depths of earthquakes showing reverse faulting (three events) are restricted between 12 and 14.0 km, but the depths of those with strike-slip faulting (7 events) are spread between 5.5 and 11.1 km. The data are few, but seem to suggest that reverse faulting occurs at greater depth than strike-slip faulting (see Figs 6–8). This pattern has been also observed around the Minab Fault located at the eastern termination of the Zagros (Yamini-Fard 2003). These data suggest that the shortening is accommodated differently in the upper crust (along strike-slip faults) from that in the lower crust. This implies a partitioning of deformation with depth: in the relatively strong, brittle upper crust, deformation is localized on pre-existing faults, but lower in the crust, deformation may occur more easily, and shortening is accommodated by reverse dip-slip faulting perpendicular to the shortening direction.

Sense of slip on the active faults

The strike-slip fault mechanisms located to the east, near the Dena Fault, consistent show right-lateral motion on NNW–SSE striking faults, and mechanisms of earthquakes in the western region are consistent with right-lateral motion on WNW–ESE striking faults (Fig. 9). This pattern of strike-slip faulting suggests a transfer of the right-lateral motion from the Dena–Kazerun–Borazjan fault system to the Ardal Fault. We cannot confirm the details of transfer of motion at the end of the Main Recent Fault proposed by Authemayou *et al.* (2005), because we observe only little microearthquake seismicity located east of the Kazerun Fault system (i.e. the Dena Fault) and associated with the Semirom Fault.

The orientation average azimuth of the *P* axes of N8°E is close to the orientation of convergence between Arabia and Central Iran obtained by GPS measurements (Tatar *et al.* 2002).

CONCLUSION

The seismicity recorded during 2 months in the region near the intersection of the Kazerun fault system and the Main Recent Fault confirms that:

(1) the velocity structure in this area is different from that in Central Zagros, because the thickness of sedimentary rock is less (∼6–8 km instead of 11 km), and *P* and *S* wave speeds are slightly higher, suggesting a different evolution of the sedimentary cover.

(2) the crustal thickness is similar on both sides of the Kazerun Fault consistent with pure strike slip between 2 blocks of similar thickness and no thickening across the fault.

(3) the MZRF is not seismically active and does not accommodate deformation as evidenced also by GPS.

(4) the seismically active area lies in the region surrounded by the Main Recent, Dena, and High Zagros Faults, but the locations do not define individual faults,

(5) slip associated with the Dena Fault is right-lateral strike-slip, as it is for the Ardal Fault,

(6) the most active reverse faults seem to be the Dopolan and the Gazulak faults, which form the eastern termination of the High Zagros Fault and were the probable location of the destructive 1977 Naghan earthquake.

(7) we observe little seismic activity around the Semirom Fault located east of the Dena Fault.

(8) On the other hand our partitioning of focal mechanisms with depth suggests that the upper crust and the lower crust accommodate the shortening differently.

The upper crust is stronger, faults surround undeformable blocks and concentrate the deformation, but the lower crust accommodates the shortening more simply with reverse faults striking perpendicular to the orientation of shortening.

ACKNOWLEDGMENTS

This study was supported by IIEES (International Institute of Earthquake Engineering and Seismology), INSU-CNRS (Intérieur de la Terre) and the French Ministère des Affaires Etrangères in the frame of a cooperative research program. We thank M. Ghafory-Ashtiany, president of IIEES, for his support. We thank the IIEES team for support, administrative and field work assistance including M. Masoudi, M. Zolfaghari, M. Ghasemi, A. Fatehi, and G. Javan-Doloei. We had fruitful discussions with C. Authemayou, M. Berberian, J. Jackson and P. Molnar. Constructive reviews by O. Bellier and an anonymous reviewer contributed to improve the manuscript. This work would not have been possible without the help of the people of the Chahar Mahale Bakhtiari province and especially the local governor of Borujen.

REFERENCES

Ambraseys, N.N. & Melville C.P., 1982. A history of Persian earthquakes, Cambridge Earth Science Series, Cambridge University Press, London, pp. 212.

Authemayou, C., Bellier, O., Chardon, D., Malekzadeh, Z. & Abbassi, M., 2005. Role of the Kazerun Fault system in active deformation of the Zagros Fold-and-Thrust belt (Iran), C. Acad. Sci., *Geoscience,* **337,** 539–545.

Authemayou, C., Chardon, D., Bellier, O., Malekzade, Z., Shabanian, E. & Abbassi, M.R., 2006. Oblique convergence and partitioning within the Zagros thrust-fold belt: the role of the Kazerun and Main recent faults (Southern Iran), *Tectonics*, in press.

Baker, C., 1993. The active seismicity and tectonics of Iran, *PhD thesis*, University of Cambridge, UK, p. 228.

Baker, C., Jackson, J. & Priestly, K., 1993. Earthquakes on the Kazerun Line in the Zagros Mountains of Iran: strike-slip faulting within a fold-and-thrust belt, *Geophys. J. Int.,* **115,** 41–61.

Berberian, M., 1995. Master blind thrust faults hidden under the Zagros folds: active basement tectonics and surface morphotectonics, *Tectonophysics,* **241,** 193–224.

Berberian, M. & Navai, I., 1977. Naghan (Chahar Mahal Bakhtiari-High Zagros, Iran) Earthquake of April 1977: a preliminary report and seismotectonic discussion, *Geol. Surv. of Iran*, Report No. 40.

Engdahl, E.R., Van Der Hilst, R. & Buland, R., 1998. Global teleseismic earthquake relocation with improved travel-times and procedures for depth determination, *Bull. Seismol. Soc. Am.,* **88,** 722–743.

Falcon, N.L., 1969. Problem of relationship between surface structure and deep displacements illustrated by the Zagros Range. eds Kent, P.E., Satterthwaite, G.E. & Spencer, A.M., Time and place Orogeny, *Geol. Soc. London, Spec. Publ.,* **3,** 9–22.

Falcon, N., 1974. Southern Iran: Zagros Mountains, in *Mesozoic-Cenozoic Orogenic Belts*, edited by Spencer, *Spc. Publ. Geol. Soc.* London, **4**, pp. 199–211.

Fitch, T., 1972. Plate convergence, transcurrent faults, and internal deformation adjacent to southeast Asia and the western Pacific, *J. geophys. Res.,* **84,** 4432–4460.

Hatzfeld, D., Tatar, M., Priestly K. & Ghafory Ashtiani M., 2003. Seismological constraints on the crustal structure beneath the Zagros Mountain belt (Iran). *Geophys. J. Int.,* **155,** 1–8.

Kaviani, A., 2004. La chaıne de collision continentale du Zagros (Iran): Structure lithosphérique par analyse de données sismologiques. *Thèse de l'Université Joseph Fourier*, Grenoble, France.

Kissling, E., 1988. Geotomography with local earthquake data, *Rev. of Geophys.,* **26,** 659–698.

Koop, W.J. & Stoneley, R., 1982, Subsidence history of the Middle East Zagros Basin, Permian to Recent, *Phil. Trans. R. Soc. Lond.,* **305,** 149–168.

Lee, W.H.K. & Lahr J.C., 1975. HYPO71 (Revised): a computer program for determining hypocenter, magnitude, and first motion pattern of local earthquakes, *U. S. Geological Survey, Open File Report*, 75–311.

Ligorria, J. & Ammon, C., 1999. Iterative deconvolution and receiver function estimation, *Bull. Seism. Soc. Am.,* **89,** 1395–1400.

McCaffrey, R., 1992. Oblique plate convergence, slip vectors, and fore-arc deformation, *J. geophys. Res.,* **97,** 8905–8915.

Maggi, A., Jackson, J.A., Priestley, K. & Baker, C., 2000. A reassessment of focal depth distributions in Southern Iran, the Tien Shan and Northern India; Do earthquakes really occur in the continental mantle?, *Geophys. J. Int.,* **143,** 629–661.

Richard, P. & Cobbold, P., 1989. Structures en fleur positives et décrochements crustaux: modélisation analogique et interpretation mécanique, *C.R. Acad. Sci.,* **308,** 553–560.

Ricou, L.E., Braud, J. & Brunn J.H., 1977. Le Zagros, *Mém. Soc. Géol. Fr.,* **8,** 33–52.

Stöcklin, J., 1968. Structural history and tectonics of Iran, a review, *Am. Assoc. Pet. Geol. Bull.,* **52,** 1229–1258.

Talebian, M. & Jackson, J., 2002. Offset on the Main Recent Fault of NW Iran and implications for the late Cenozoic tectonics of the Arabia-Eurasia collision zone, *Geophys. J. Int.,* **150,** 422–439.

Talebian, M. & Jackson, J., 2004. A reappraisal of earthquake focal mechanisms and active shortening in the Zagros mountains of Iran, *Geophys. J. Int.,* **156,** 506–526.

Tatar, M., Hatzfeld, D., Martinod, J., Walpersdorf, A., Ghafory-Ashtiany, M. & Chéry, J., 2002. The present-day deformation of the central Zagros from GPS measurements, *Geophys. Res. Lett.,* **29**(19), doi:10.1029/2002GL015159.

Tatar, M., Hatzfeld, D. & Ghafory-Ashtiany, M., 2004. Tectonics of the Central Zagros (Iran) deduced from microearthquake seismicity, *Geophys. J. Int.,* **156,** 255–266.

Tchalenko, J.S. & Braud J., 1974. Seismicity and structure of the Zagros (Iran) — the main recent fault between 33 and 35° N, *Philo. Trans. Roy. Soc. London,* **277,** 1–25.

Vernant, P. *et al.*, 2004. Contemporary crustal deformation and plate kinematics in the Middle East constrained by GPS measurements in Iran and Northern Oman, *Geophys. J. Int.,* **157,** 381–398.

Waldhauser, F. & Ellsworth W.L., 2000. A double-difference earthquake location algorithm: application to the northern Hayward Fault, California. *Bull. Seismol. Soc. Am.,* **90,** 1353–1368.

Walpersdorf, A. *et al.*, 2006. Difference in the GPS deformation pattern of North and Central Zagros (Iran), *Geophys. J. Int.,* submitted.

Yamini-Fard F., 2003. Sismotectonique et structure lithosphérique de deux zones de transition dans le Zagros (Iran): la zone de Minab et la zone de Qatar-Kazerun. *PhD thesis*. Joseph Fourier University—Grenoble I.